JOURNAL OF MATERIALS SCIENCE 27 (1992) 1070–1080

Nucleation on the crack tip and transformation toughness in crystals undergoing structural phase transitions

A. A. BULBICH
Research Institute of Physics, Rostov State University, Rostov-on-Don, USSR

Stress-induced local phase transition on both motionless and moving cracks is considered. The asymptotically exact solution describing a small nucleus of a new phase on a crack tip is obtained. The nucleation temperature value is determined and nuclei phase diagram is constructed on the background of a phase diagram of bulk transition. It is demonstrated that nucleation is possible only during slow subcritical crack growth. The exact solution of the phase boundary equilibria equation is obtained for the case of a large nucleus. It is shown that fracture toughness has a maximum near the transition point.

1. Introduction

The existence of stress concentrators in crystals can be the origin of new phase nuclei arising when the temperature, T_0, is higher than the temperature of a phase transition in the bulk, T_c, if the solid undergoes phase transitions (PT) under the applied stress. Nuclei affect the solid body mechanical properties related to the concentrators' behaviour – the fracture toughness, ductility, internal friction and so on.

Local (L) PT generated by cracks were observed due to the existence of a "trail" – a thin layer of a new phase on a fracture surface differing from that in the bulk of crystal. Monoclinic and orthorhombic trails were observed on the tetragonal ZrO_2 fracture surface [1, 2] a graphite trail under the thermal fracture of diamonds [3], a martensitic trail under the fatigue steel fracture [4], and a ferroelectric phase trail under the $Pb(Ti, Zr)O_3$ fracture [5].

The results of the direct evidence of the martensitic LPT on the crack tip in the martensitic–austenitic alloy Fe–28Ni–3Ti–0.6Al foil is shown in Fig. 1 which was taken using a transmission electron microscope during the process of the crack growth. The dark background indicates the martensitic phase, localized at the crack tip, b, and a trail, c, which is partially twinned.

LPT on dislocations were observed in gadolinium iron garnet [6, 7], in NH_4Br [8] and in the Ni_4Mo alloy [9].

It has been established that the nucleus arising on the crack tip is followed by an increase in fracture toughness in ZrO_2 monocrystals and ceramics [1, 2, 10, 11] and in the composites Al_2O_3–ZrO_2, ZnO–ZrO_2, Si_3N_4–ZrO_2 [12, 13] and in the high-temperature superconductor $YBa_2Cu_3O_{7-x}$–ZrO_2 [14].

The increase in fracture toughness was predicted [16] (and then further considered [11, 17–19]) from the proposition that the trail free energy density is more than that in the bulk of the crystal. The trail energy renorms the surface crack energy σ_0

$$\sigma = \sigma_0 + \rho_* \Delta f \quad (1)$$

where ρ_* is the trail width and Δf the phase free energy difference. The fracture toughness increases as [16]

$$K_{IC}^2 = \frac{2\sigma E}{1 - \nu^2} \quad (2)$$

where E is the Young's modulus and ν is Poisson's ratio. ρ_* and Δf were supposed to be independent [11, 16–19]. In this case K_{IC} becomes a maximum on the two-phase region boundary of the phase diagram. This is, however, contrary to the experimental $K_{IC}(x)$ dependence on $(ZrO_2)_{1-x}(Y_2O_3)_x$ [10, 20]. K_{IC} increases from 1.7 MN m$^{-3/2}$ at 20 wt % Y_2O_3, which corresponds to the cubic phase, to 8 MN m$^{-3/2}$ at 4 wt % Y_2O_3 (the region of tetragonal and monoclinic phases coexistence). The mean strength changed from 210 MPa at 20 wt % Y_2O_3 to 1000 MPa at 6 and 4 wt % Y_2O_3 with the maximum value 1400 MPa at 5 wt % Y_2O_3 [10]. The strength and fracture toughness thus have a maximum and decrease with distance from the PT point. The contradiction arose because the phase boundary equilibria equation (which establishes the $\rho_*(\Delta f)$ dependence) was not taken into account.

The problem of determining the conditions of a crack tip nucleus arising and a nucleus phase diagram description have not yet been investigated.

In this paper the structural LPT on the crack tip in the brittle solid is described. The nucleation temperature is determined for crystals undergoing a second-order PT as well as a first-order PT close to a second-order PT and a phase diagram of a nucleus is constructed. Anomalies of physical properties at the nucleation point are calculated. The nucleation on a moving crack tip is investigated. It is demonstrated

0022–2461

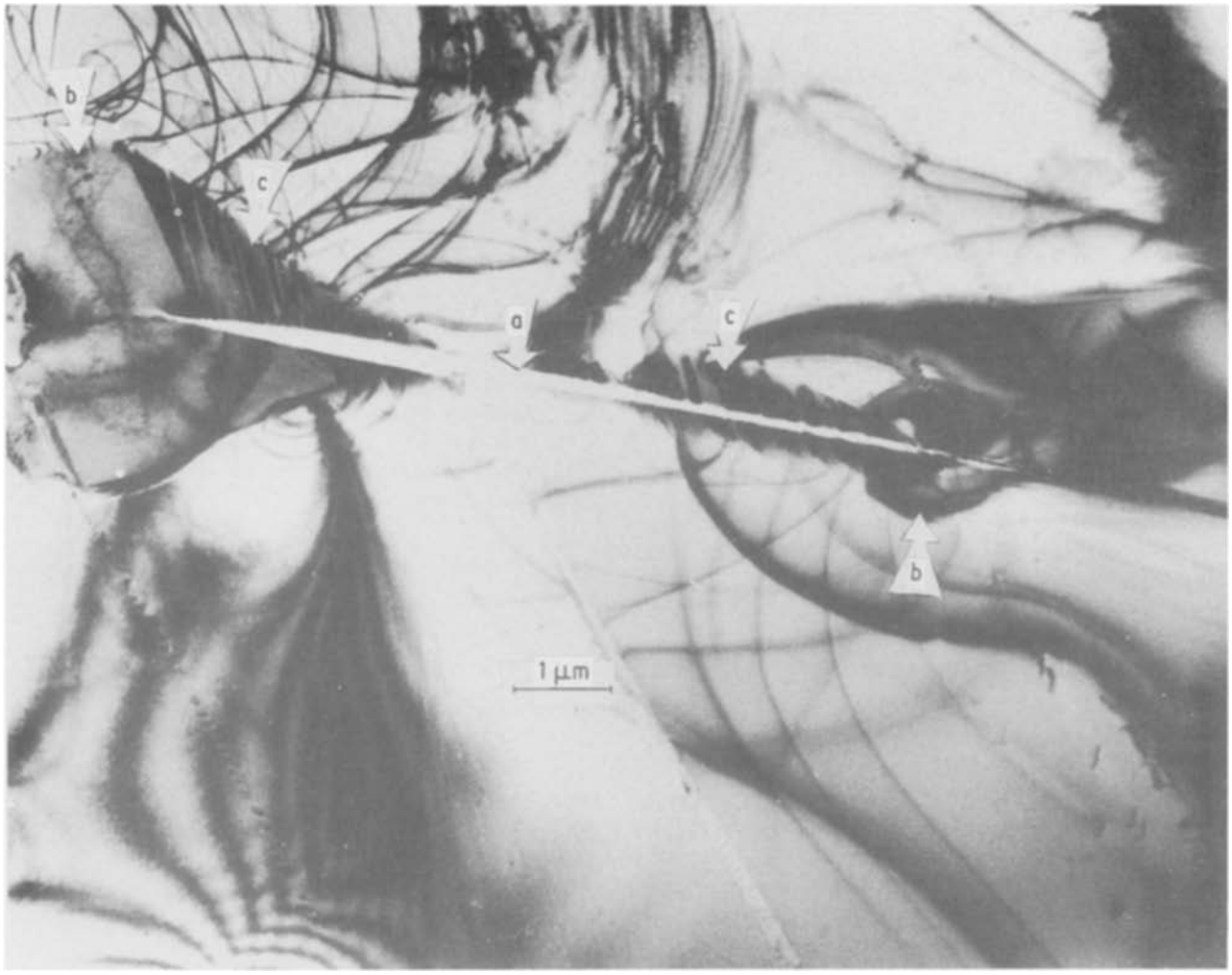

Figure 1 Local phase transition on the crack tip in the martensite–austenite Fe–28Ni–3Ti–0.6Al alloy foil. (a) The crack (b) the martensite nuclei (c) the martensite trail, which is partially twinned. Background–the austenite phase. (Reproduced with kind permission of Dr V. I. Isotov Central Black Metallurgy Research Institute, USSR)

that there is a critical value of the crack tip speed, v_c, such that if $v \geqslant v_c$ the crack tip nucleus cannot arise. The exact solution of the nucleus phase boundary equation is obtained for the case of a large nucleus and the transformation toughness is found to be a maximum near the PT point.

2. Nucleus arising on the tip of a motionless crack

Consider an elastically isotropic crystal undergoing PT with decreasing temperature or under the applied stress. In the simplest case of PT described by a one-component order parameter (OP) η, the crystal Ω potential has the form

$$\Omega = \int_v [f_{el}(u_{ik}) + f(\eta) + \tfrac{1}{2} g(\nabla\eta)^2 - A\eta^2 u_{ii}]\,dV + \int_s (\sigma_0 - p_i u_i)\,dS \qquad (3)$$

where

$$f_{el}(u_{ik}) = \tfrac{1}{2}\lambda_0 u_{ll}^2 + \mu u_{ik}^2 \qquad (4)$$

$$f(\eta) = \tfrac{1}{2}\alpha\eta^2 + \tfrac{1}{4}\beta\eta^4 + \tfrac{1}{6}\gamma\eta^6 \qquad (5)$$

$\lambda_0 = E\nu/(1 - 2\nu)(1 + \nu)$, $\mu = E/2(1 + \nu)$ are the elastic constants, u_{ik} the strain tensor, u_i the displacement vector, V the crystal volume, S the crystal surface area, p_i the force applied to the crystal surface, g, α, β and γ the phenomenological constants: $g, \gamma > 0$, but α and β can change their signs with a change of the external thermodynamic parameters, $\alpha = \alpha'(T - T_c)$, T the temperature, and A is the striction factor.*

Equation 3 describes the PT from the homogeneous phase $\eta = 0$ to the homogeneous phase η = constant in a crystal which does not contain any crack. The phase diagram of a crystal without a crack which is free of stress is shown in Fig. 2 on the plane (α, β).

If $\beta_1 = \beta - 6A^2(1 - 2\nu)/E > 0$ the second-order PT takes place on the line $\alpha = 0$ of the phase diagram. If $\beta_1 < 0$ – the first-order PT takes place on the line

* The term $\sim\eta^2 u_{ii}$ in Equation 3 leads to the spontaneous dilatation arising (which always follows PT). If PT results is the elementary cell multiplication, the other types of spontaneous deformation are absent. The exceptions are the improper ferroelastics, which are not under consideration here.

$\alpha = 3\beta_1^2/16\gamma$ (the line 1, Fig. 2). Phases coexist between the lines $\alpha = \beta_1^2/4\gamma$ (line 2, Fig. 2) and $\alpha = 0$, $\beta_1 < 0$.

Consider the infinite crystal containing the flat crack, length $2a$, situated symmetrically with respect to the coordinates origin along the Ox axis, opened by the normal force.

The state equations which follow from the minimum conditions of functional 3 are

$$\begin{aligned} g\Delta\eta &= (\alpha - 2Au_{ll})\eta + \beta\eta^3 + \gamma\eta^5 \\ \frac{\partial\sigma_{ik}}{\partial x_k} &= 0 \\ \sigma_{ik} &= \lambda_0 u_{ll}\delta_{ik} + 2\mu u_{ik} - A\eta^2\delta_{ik} \qquad (6) \\ \sigma_{ik}n_k &= p_i(t) \quad t\in L \end{aligned}$$

where $\Delta = \partial^2/\partial x^2 + \partial^2/\partial y^2$, σ_{ik} is the stress tensor, L the crack contour and n_k the normal unit. The boundary condition $\sigma_{yy} = -p(t)$, $t\in L$ corresponds to the case of the normal force applied to the crack surface.

When considering the problem of a nucleus arising, one has to demand $\eta(\infty) = 0$. Besides, OP is limited everywhere, due to it's physical origin.

The reason for a nucleus of a phase $\eta \neq 0$ arising on the background of a phase $\eta = 0$ is the "local Curie temperature" decreasing near the crack tip: the factor multiplying η^2 can be written as $\alpha_{ef} = \alpha'(T - T_c(r,\theta))$, where $T_c(r,\theta) = T_c - 2Au_{ii}(r,\theta)/\alpha'$ is the "local Curie temperature". The $\alpha_{ef}(r,\theta) = 0$ condition gives a rough nucleus size estimation* if the gradient terms in (3) are neglected. The solution of the equation $r = r(\theta) > 0$ exists if $A > 0$ – this will be assumed in the rest of the paper.

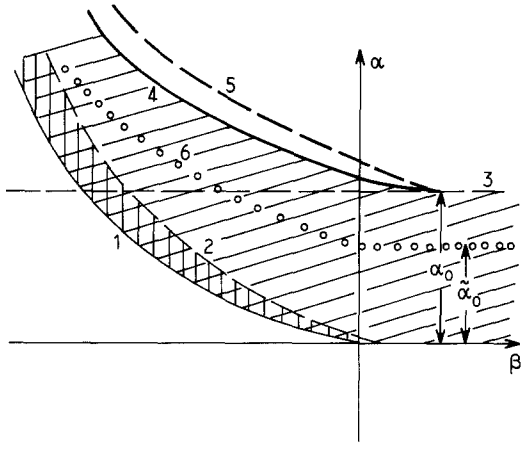

Figure 2 Phase diagram of nucleation on the crack tip on the background of phase diagram of transition in the bulk of crystal. 1. The energy equality line of the bulk phases $\eta = 0$ and $\eta \neq 0$ (the first-order phase transition line). 2. The instability line for the phase $\eta \neq 0$ (for the first-order transition in the bulk). 3. The line $\alpha = \alpha_0$. 4. The line of energy equality of a crack with nucleus and a crack without nucleus $\Omega(\xi) = \Omega_0$. 5. The instability line for the solution $\xi \neq 0$. 6—the transition line in the case of moving crack.

At high temperatures (large values of α) Equation 6 has the solution

$$\begin{aligned} \eta &= 0 \\ \sigma_{ik}^{(0)} &= \frac{K_I}{(2\pi r)^{1/2}} f_{ik}(\theta) \qquad (7) \end{aligned}$$

where

$$K_I = \frac{1}{(\pi a)^{1/2}} \int_{-a}^{a} \left(\frac{a+x}{a-x}\right)^{1/2} p(x)\,dx \qquad (8)$$

is the stress intensity factor; r and θ are the cylindrical coordinates counted off the crack tip, $f_{ik}(\theta)$, the well known stress angle dependence [15]. Its trace is $f_{ll}(\theta) = 2\cos(\theta/2)$.

If, however, α becomes smaller then α_0, the first eigenvalue of the equation

$$\begin{aligned} g\Delta\Psi_n &= \left(\alpha_n - B\frac{\cos(\theta/2)}{r^{1/2}}\right)\Psi_n \qquad (9) \\ B &= \frac{4AK_I(1-2\nu)(1+\nu)}{(2\pi)^{1/2}E} \end{aligned}$$

the small solution

$$\eta = \xi\Psi_0(r,\theta) \quad \sigma_{ik} = \sigma_{ik}^{(0)} + O(\xi^2) \qquad (10)$$

branches off (Equation 7). Here Ψ_0 is the eigenfunction corresponding to α_0. The amplitude ξ is to be determined.

The exact solution of the anisotropic Shrödinger equation 9 is interesting in itself and is given in Appendix 1.

The result is

$$\alpha_0 = \frac{1}{16^{1/3}}\left(\frac{2K_IA(1-2\nu)(1+\nu)}{g^{1/4}E}(2/\pi)^{1/2}\right)^{4/3} \qquad (11)$$

$$\psi_0 = \frac{1}{(s_2(0))^{1/2}}\exp\left[-\frac{r}{(4)^{1/3}r_0} + (4)^{1/3} \times \left(\frac{r}{r_0}\right)^{1/2}\cos(\theta/2)\right] \qquad (12)$$

where the normalization factor $s_2(0) \approx 175$

$$r_0 = \left(\frac{gE}{2AK_I(1-2\nu)(1+\nu)}(\pi/2)^{1/2}\right)^{2/3} \qquad (13)$$

is the nucleus radius.

The branching point value (Equation 11) is obtained as a result of the exact solution (Appendix 1) and gives the exact nucleation temperature value T_0 as $\alpha_0 = \alpha'(T_0 - T_c)$. However, Equations 10 and 12, give the main term of the solution of Equation 6 and have to be considered asymptotically exact if the amplitude ξ is small enough.

The OP distribution corresponding to the nucleus on the motionless crack tip (Equations 10 and 12) is displayed in Fig. 3a. Substitution of the solution (Equation 10) into the functional (Equation 3) gives

* This estimation is true in the region of developed nucleus existence $r_0 \gg r_c$, where r_0 is the nucleus size as $r_c \sim (g/\alpha)^{1/2}$ the correlation radius. In Sections 1–4 the case of the nucleus arising and close overcritical regime $r_0 \sim r_c$ is considered. In this case the estimation can give only the sign of A.

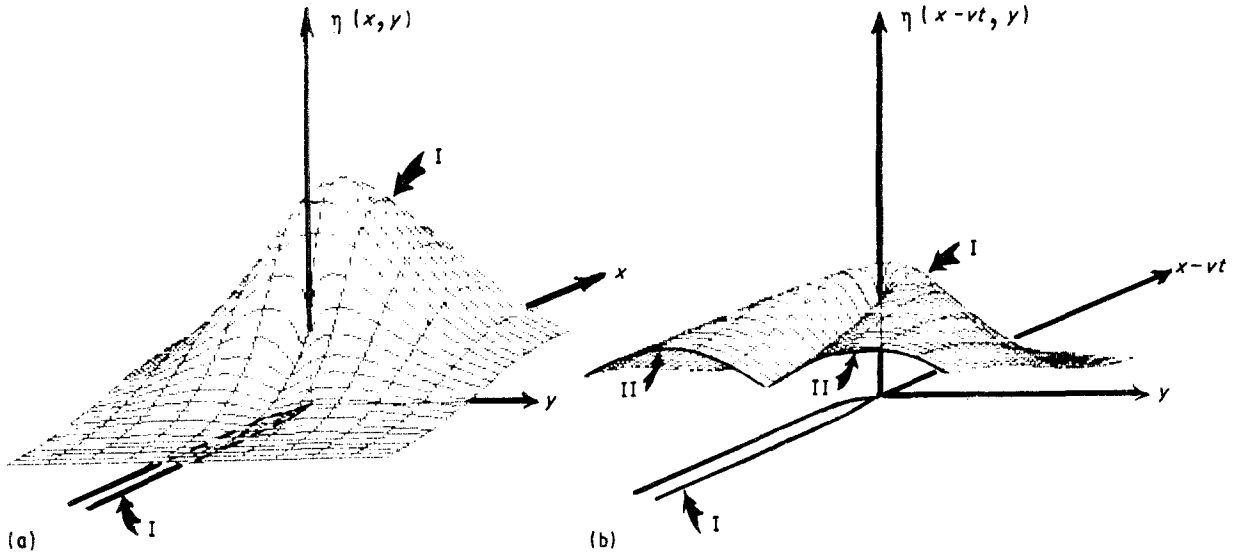

Figure 3 The order parameter $\eta(x, y)$ distribution at the tip of (a) motionless crack (10, 12) (b) moving crack (22). I the crack, II the nucleus, III the unstable trail. The amplitudes were chosen to be equal during (a) and (b) distribution construction.

the Ω potential of the crack with the nucleus

$$\Omega(\xi) = \Omega_0 + r_0^2 l\left(\frac{1}{2}(\alpha - \alpha_0)\xi^2 + \frac{0.018}{4}\tilde{\beta}\xi^4 + \frac{0.00048}{6}\gamma\xi^6\right) \quad (14)$$

where l is the crystal length in the Oz direction and Ω_0 the mechanical and surface crack energy

$$\tilde{\beta} = \beta - \frac{A^2(1 - 2\nu)(1 + \nu)}{E(1 - \nu)}[2 + 0.77(1 - 2\nu)] \quad (15)$$

The potential (Equation 14) is obtained in Appendix 2.

3. Phase diagram of nucleus on the motionless crack tip

The Ω potential (Equation 14) describes the PT from the state without a nucleus ($\xi = 0$) to the state $\xi \neq 0$ corresponding to the nucleus existing on the crack tip ($\xi \neq 0$). ξ plays the role of OP in this transition. It has be determined from the minimum conditions of (Equation 14): $\partial\Omega/\partial\xi = 0$; $\partial^2\Omega/\partial\xi^2 > 0$.

If $\tilde{\beta} > 0$ the six-order term in (Equation 14) can be neglected and

$$\xi^2 = \begin{cases} 0 & \alpha > \alpha_0 \\ -56(\alpha - \alpha_0)/\tilde{\beta} & 0 < \alpha < \alpha_0 \end{cases} \quad (16)$$

If $\tilde{\beta}$ is small by its absolute value and negative

$$\xi^2 \approx 18.8\frac{|\tilde{\beta}| + [\tilde{\beta}^2 - 5.9\gamma(\alpha - \alpha_0)]^{1/2}}{\gamma} \quad (17)$$

The nucleus phase diagram is drawn on the background of the phase diagram of the transition in the bulk of the crystal (Fig. 2).

If $\tilde{\beta} > 0$ the nucleation takes place on the line $\alpha = \alpha_0$ (line 3, Fig. 2) by way of second-order PT. If $\tilde{\beta} < 0$, the real solution of (Equation 17) appears below the line $\alpha \approx \alpha_0 + 0.17\tilde{\beta}^2/\gamma$ (line 5, Fig. 2). $\Omega(\xi) > \Omega_0$ here, however, and the state without a nucleus is thermodynamically advantageous. $\Omega(\xi) = \Omega_0$ on the line $\alpha \approx \alpha_0 + 0.13\tilde{\beta}^2/\gamma$ (line 4, Fig. 2), below this line the state with a nucleus is thermodynamically advantageous. The shaded region is the phase diagram region of nuclei existence. Lines 1 and 4 intersect but the intersection point lies far from the region where this theory can be used.

The observable nucleus size increases continuously if $\tilde{\beta} > 0$, being equal to zero on the line $\alpha = \alpha_0$. If $\tilde{\beta} < 0$, however, the nucleus arises on line 5, with finite value of ξ and of observable size. The nucleus size grows with decreasing temperature and occupies the whole crystal when the line $\alpha = 0$, $\beta_1 > 0$ or the line 1, $\beta_1 < 0$ is reached.

Such behaviour demonstrated nuclei on dislocations in iron garnet [6, 7].

4. Nucleation on the tip of a moving crack

The nucleus phase diagram and nearly overcritical nucleus regime on the motionless crack tip is described above. In order to understand nuclei fracture influence, it is necessary, however, to investigate nucleation on a moving crack tip.

If $v/c \ll 1$ (here v is the crack tip speed and c the speed of sound in the crystal), the stress distribution is close to that near the motionless crack tip in the coordinate system moving with the crack [22].

The dynamic equation for OP is

$$k\frac{\partial\eta}{\partial t} = g\Delta\eta - (\alpha - 2Au_{ii}(\zeta, y))\eta - \beta\eta^3 - \gamma\eta^5 \quad (18)$$

if the thermometric conductivity is much greater than g/k, where $k > 0$ is the kinetic factor, $\zeta = x - vt$; the coordinate origin is in the right crack tip. The term $\partial^2\eta/\partial t^2$ which is usually taken into account in

TABLE I
VAULES OF $s_n(\delta)$
$\delta = r_0 kv/2g$

$$s_2(\delta) = \int_0^\infty \int_{-\pi}^{\pi} \exp\{-2\delta\rho\cos\theta - 2\rho/4^{1/3} + 2(4)^{1/3}\rho^{1/2}\cos(\theta/2)\}\rho\,d\rho\,d\theta$$

$$s_2'(\delta) = \int_0^\infty \int_{-\pi}^{\pi} \frac{\cos(\theta/2)}{r_1^{1/2}} \Phi_\delta^2(r_1, \theta) r_1\,dr_1\,d\theta;$$

$$s_n(\delta) = \int_0^\infty \int_{-\pi}^{\pi} \Phi_\delta^2(r_1, \theta) r_1\,dr_1\,d\theta/r_0^2 \quad (n = 4, 6)$$

s	δ								
	0	0.1	0.2	0.3	0.4	0.5	0.6	0.61	0.62
s_2	174.7	112.3	85.0	75.3	81.4	12.5	871.7	1352	3102
s_4	0.018	0.020	0.020	0.019	0.014	0.008	0.001	6×10^{-4}	3×10^{-4}
$s_6\times10^{-5}$	47	61	65	55	33	9.6	0.17	0.057	0.013
s_2'	0.53	0.55	0.54	0.50	0.42	0.29	0.078	0.055	0.034
s_4^2/s_6	0.69	0.66	0.65	0.65	0.59	0.59	0.59	0.63	0.60

Equation 18 can be neglected here due to low crack speed (as shown by the estimations in Section 9).

A solution of Equation 19 of the form $\eta = \eta(\zeta, y)$ should be tried. The non-trivial solution (Equation 19) branches off the solution $\eta = 0$ if $\alpha \leqslant \tilde{\alpha}_0$ the first eigenvalue of the equation

$$g\left(\frac{\partial\Phi_n}{\partial\zeta^2} + \frac{\partial^2\Phi_n}{\partial y^2}\right) + kv\frac{\partial\Phi_n}{\partial\zeta} - \left(\tilde{\alpha}_n - B\frac{\cos^{\theta/2}}{(\zeta^2 + y^2)^{1/4}}\right)\Phi_n = 0 \qquad (19)$$

It is

$$\tilde{\alpha}_0 = \alpha_0 - \frac{k^2v^2}{4g} \qquad (20)$$

α_0 is given by Equation 11. The branched-off solution is

$$\eta = \frac{\xi}{(s_2(\delta))^{1/2}} \exp\left(-\frac{kv}{2g}\zeta\right)\Psi_0(r_1, \theta) \qquad (21)$$

Ψ_0 is given by expression 12, but in Equation 12 r must be replaced by $r_1 = (\zeta^2 + y^2)^{1/2}$. $s_2(\delta)$ is the normalization factor, $\delta = r_0 kv/2g$. The OP distribution (Equation 21) is shown in Fig. 3b.

One can see, that if $v = v_c$, where

$$v_c^2 = \frac{4g\alpha_0}{k^2} \qquad (22)$$

$\tilde{\alpha}_0 = 0$, so if $v \geqslant v_c$ the nucleation on the crack tip is impossible. That is why transformation toughness can be realized only during slow subcritical crack growth.

The equation of state for the amplitude ξ can be found by the same method used for the case of the motionless crack (Appendix 2). The Ω potential of the crack has the form

$$\Omega(\xi) = \Omega_0 + r_0^2 l\left(\frac{1}{2}(\alpha - \tilde{\alpha}_0)\xi^2 + \frac{s_4(\delta)}{4}\beta\xi^4 + \frac{s_6(\delta)}{6}\gamma\xi^6\right) \qquad (23)$$

in the $A^2/E \ll 1$ case. Here

$$s_n(\delta) = \int_0^\infty \int_{-\pi}^{\pi} \Phi_0^n(r_1, \theta) r_1\,dr_1\,d\theta/r_0^2.$$

The values of $s_n(\delta)$ for different values of $v < v_c$ are given in Table I. (v_c corresponds to $\delta_c = 4^{-1/3} \approx 0.63$.)

If $\beta > 0$ second-order PT takes place on the line $\alpha = \tilde{\alpha}_0$ ($\tilde{\alpha}_0 < \alpha_0$), but if $\beta < 0$ the first-order PT takes place on the line $\alpha = \tilde{\alpha}_0 + 3(s_4(\delta))^2\beta^2/(16 s_6(\delta)\gamma)$ (line 6, Fig. 2).

Table I makes it clear that the value $(s_4(\delta))^2/s_6(\delta)$ weakly depends on δ, so the transition line for the nucleation on the moving crack tip repeats that for the motionless crack and lies below it.

5. Two kinds of trails

The OP distribution (Fig. 3b) is stretched towards the direction opposite to the speed of the crack tip (in comparison to OP distribution on the motionless crack). The nucleus size in this direction

$$L_t = \left(\frac{1}{(4)^{1/3}r_0} - \frac{kv}{2g}\right)^{-1}$$

becomes infinite if $v \Rightarrow v_c - 0$. Let us call this part of OP distribution, the trail.

This trail is unstable. It arises because of slow OP relaxation in the indicated region of crystal.

Another kind of trail is, however, possible in the case of first-order PT – the metastable trail.

The region of existence of nuclei on a crack tip overlaps with the region of phase diagram of the homogeneous crystal in which phases $\eta = 0$ and η = constant coexist, but the phase $\eta = 0$ is thermodynamically advantageous (the double shaded part of the phase diagram, Fig. 2). The inequality $\xi(\delta) > \eta_1$ is true in this region (here $\xi(\delta)$ is the solution of the state equation which follows from the minimum condition of the potential (Equation 22), η_1 is that value of the OP which gives a maximum to $f(\eta)$ (Equation 5), Fig. 4). This inequality realization results in OP

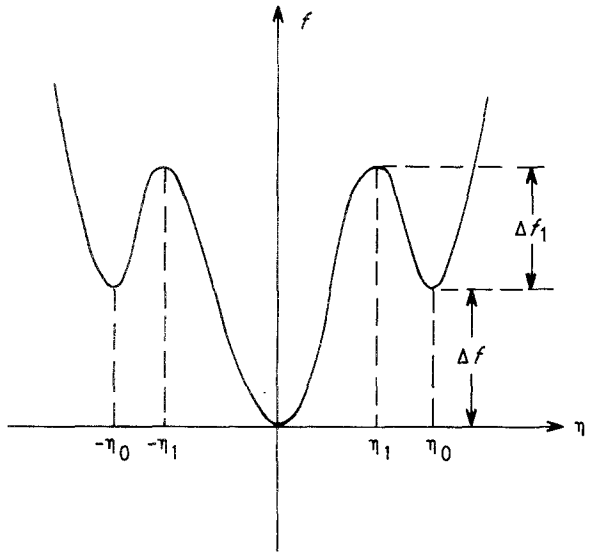

Figure 4 Density of Ω-potential dependence on order parameter in the two-phase region of phase diagram.

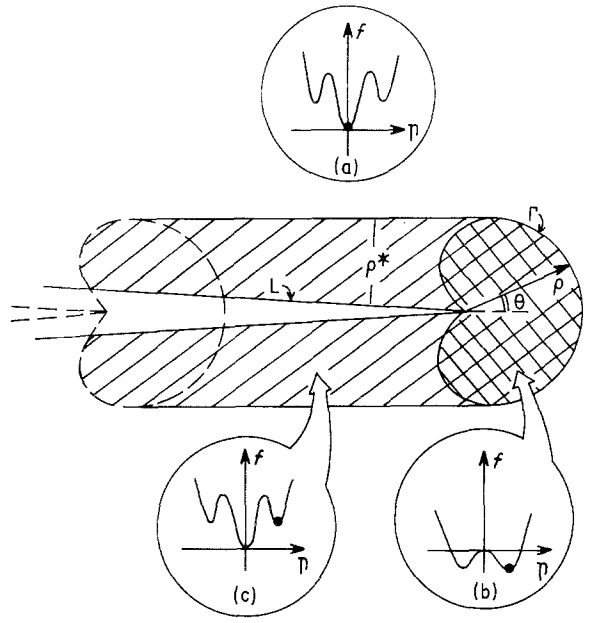

Figure 5 A metastable trail arising. Shaded is the trail, twice shaded-is the nucleus on the crack tip. (a) The order parameter dependence of Ω-potential density in the bulk of a crystal. (b) In the nucleus. (c) In the trail. The point marks the state which is realized.

relaxation to the OP vaue $\eta = \eta_0$ after the crack tip displacement. The layer of phase $\eta = \eta_0 =$ constant in the metastable state is left behind the crack – it is the metastable trail (Fig. 5). The time τ of a metastable trail decay depends on a barrier value $\tau \sim \exp(-\Delta f_1/T)$ (Fig. 4) and can be large far from the tricritical point ($\alpha = \beta = 0$).

It is necessary to expand some additional energy in order to create a metastable trail behind the moving crack tip. This energy renorms surface crystal energy and increases fracture toughness (1, 2). Near the branching point, this contribution is small (as well as nucleus size). A large contribution to strength can be obtained in the case of the developed nucleus $r_0 \gg r_c$. In order to obtain this contribution it is necessary to know the nucleus shape and size in the far overcritical regime.

6. The equation of state of nucleus in far overcritical regime

In the case of a large nucleus $r_0 \gg r_c$ the gradient term in Equation 3 can be neglected. It results in the crystal separating into the region V^+ (the region of the phase $\eta \neq 0$ localization) and V^- (phase $\eta = 0$ localization region) with unknown phase boundary. The Ω potential of the crystal gains the form

$$\Omega = \int_{V^+} (f(\eta) + f_{el}(u_{ik}) - A\eta^2 u_{ii})\,dV^+ + \int_{V^-} f_{el}(u_{ik})\,dV^- - \int_S P_i u_i\,dS \qquad (24)$$

The phase boundary Γ (Fig. 5) can be coherent as well as incoherent. The coherence failure (which occurs by twinning and boundary dislocations generation) is a relatively slow process [22], so it is reasonable to consider the LPT on the crack tip as a transition with a coherent phase boundary: $[u_i]_{|\Gamma} \equiv (u_i^+ - u_i^-)_{|\Gamma} = 0$. Here the signs "$\pm$" are used to mark the quantity values on both phase boundary Γ sides. It should be noted that the coherent phase boundary problem can be considered in the framework of flat elasticity theory only in the case of a thin plate, because the finite constant spontaneous deformation u_{33} value in V^+ region leads to a large shear stress σ_{12} and σ_{13} on Γ arising when the crystal length in the Oz direction is large enough. It results in coherency failure or the problem being unflat. In order to arrive at the thin plate case one has to change λ_0 and A to $\lambda = 2\mu\lambda_0/(\lambda_0 + \mu)$; $A_1 = 2\mu A/(\lambda_0 + \mu)$.

The state equations may be obtained by the way of functional (Equation 24) varying by OP η and by the displacement vector u_i

$$\begin{aligned} \frac{\partial f}{\partial \eta} - 2A_1 \eta u_{ll} &= 0 \\ \frac{\partial \sigma_{ik}}{\partial x_k} &= 0 \\ \sigma_{ik} &= \lambda u_{ll}\delta_{ik} + 2\mu u_{ik} - A_1\eta^2\delta_{ik} \\ \sigma_{ik} n_{k|_S} &= P_i \end{aligned} \qquad (25)$$

and by the phase boundary Γ position

$$[\sigma_{ik}]n_{k|\Gamma} = 0 \quad [f]_{|\Gamma} - \tfrac{1}{2}\{\sigma_{ik}^+ + \sigma_{ik}^-\}[u_{ik}]_{|\Gamma} = 0 \qquad (26)$$

[23, 24]. In (Equation 26) $[f] = (f^+ - f^-)_\Gamma$, f^+ is the density value of the first term f^- – the density value of the second term in (Equation 24) on Γ. Equations 25 are fulfilled in the region V^+. The analogous system for V^- can be obtained from (Equation 25) if η is equated to zero.

In the case of phase transitions of a manifested first-order the OP has a jump in a PT point, however, it further increases with decreasing temperature and is often small and can be neglected. The case under consideration here is $\eta = \eta_0$ in the V^+ region and

$\eta = 0$ in the V^- region. The elastic constant changes in PT point will also be neglected. These assumptions are correct for most ferroelectrics [25], as well as for a lot of other crystals which undergo PT of a manifested first-order PT [26].

Equations 25 and 26 make it possible to obtain the exact solution of a problem of determination of the shape and size of a nucleus on the crack tip in the far overcritical regime.

6. The phase boundary

It has been shown that for the state equations (Equation 25) in the flat problem framework the stressed state can be described by the Airy function, which is biharmonic in the region V^+ as well as in the region V^- [28, 29]. The displacements and stresses can be expressed in terms of Kolosov–Muskhelishvily potentials $\varphi(z)$ and $\psi(z)$ [30] – the functions of the complex coordinate $z = x + iy$ in a form [29]*

$$2\mu(u + iv) = \begin{cases} \kappa\varphi(z) - z\overline{\varphi'(z)} - \overline{\psi(z)} & \text{in the phase } \eta = 0 \\ \kappa\varphi(z) - z\overline{\varphi'(z)} - \overline{\psi(z)} - Cz & \text{in the phase } \eta = \eta_0 \end{cases} \quad (27)$$

$$\sigma_{xx} + \sigma_{yy} = 4\mathrm{Re}\,\varphi'(z); \sigma_{yy} - \sigma_{xx} + 2i\sigma_{xy} = 2(\bar{z}\varphi'(z) + \psi'(z)); \quad (28)$$

$$i\int_{s(t_0)}^{s(t)} (X_n + iY_n)\,ds = \varphi(t) + \overline{t\varphi'(t)} + \overline{\psi(t)} \quad t \in L \quad (29)$$

Here "—" denotes complex conjugation, the prime means differentiation by z, $X_n + iY_n$ – the force acting to the contour L, $s(t)$ the contour arc, $\kappa = (\lambda + 3\mu)/(\lambda + \mu) = 3 - 4\nu$; u and v the displacement vector components. The last term in Equation 27 for the phase $\eta = \eta_0$ distinguishes Equations 27 to 29 from the standard flat elasticity theory formulae [30]. It describes the spontaneous deformation due to the PT: $C = -\mu A_1 \eta_0^2/(\lambda + \mu)$.

The normal stress (Equation 29) continuity condition on Γ (Equation 26) gives the equation

$$[\varphi(t) + \overline{t\varphi'(t)} + \overline{\psi(t)}] = 0 \quad t \in \Gamma \quad (30)$$

while the displacement continuity condition gives

$$[\kappa\varphi(t) - \overline{t\varphi'(t)} - \overline{\psi(t)}] = -Ct \quad t \in \Gamma \quad (31)$$

One can obtain from Equations 30 and 31 the potential jumps on Γ

$$[\varphi(t)] = \frac{C}{\kappa + 1} t \quad [\psi(t)] = -\frac{2C}{\kappa + 1}\bar{t} \quad t \in \Gamma \quad (32)$$

The integration Equations 32 with the kern $[2\pi i(t - z)]^{-1}$ gives

$$\varphi(z) = \begin{cases} \varphi_*(z) & z \in V^- \\ \varphi_*(z) + \dfrac{C}{\kappa + 1} z & z \in V^+ \end{cases} \quad (33)$$

$$\psi(z) = \psi_*(z) - \frac{2C}{\kappa + 1} I(z) \quad (34)$$

Here $\varphi_*(z)$ and $\psi_*(z)$ are continuous on Γ functions

$$I(z) = \frac{1}{2\pi i}\oint_\Gamma \frac{\bar{t}}{t - z}\,dt \quad (35)$$

Integral (35) cannot be calculated unless contour Γ is unknown because $\bar{t}$ is in a common situation a non-analytical function – its structure (the number and orders of poles, the branching points existence) depends on the Γ shape.

$\varphi_*(z)$ and $\psi_*(z)$ can be obtained from the boundary conditions on the crack contour L. If the displacements $u(t) + iv(t) = g(t)$ are given on L, one can obtain, using Equations 34 and 35 and the first Equation 27

$$\kappa\varphi_*(t) - \overline{t\varphi_*'(t)} - \overline{\psi_*(t)} = 2\mu g(t) + \frac{2C}{\kappa + 1} I(z) \quad t \in L \quad (36)$$

if the force value

$$i\int_{s(t_0)}^{s(t)} (X_n + iY_n)\,ds = f(t)$$

is given on the crack contour, it can be obtained from Equations 29, 33 and 35

$$\varphi_*(t) + \overline{t\varphi_*'(t)} + \overline{\psi_*(t)} = f(t) + \frac{2C}{\kappa + 1} I(t) \quad t \in L \quad (37)$$

Equations 36 and 37 lead to the equation for $\varphi_*(z)$

$$\varphi_*'(z) = \varphi_0'(z) + \frac{C}{\pi i(\kappa + 1)(z^2 - a^2)^{1/2}} \times \int_L \frac{(t^2 - a^2)^{1/2}}{t - a} I'(t)\,dt \quad (38)$$

The second term in Equation 38 arises due to the nucleus elastic image in the crack contour $\varphi_0(t)$ is determined by the displacement $g(t)$ or force $f(t)$ distribution on the crack contour. For example, in the boundary problem (Equation 37) case

$$\varphi_0'(z) = \frac{1}{2\pi i(z^2 - a^2)^{1/2}} \int_{-a}^{a} \frac{(t^2 - a^2)^{1/2}}{t - z} f'(t)\,dt$$

Supposing $z = a + \rho\exp(i\theta)$, $(\rho/a \ll 1)$ considering the normal force case $X_n = 0$, $Y_n = -p(t)$ and using (Equation 8) one can obtain

$$\mathrm{Re}\,\varphi_0'(z) = \frac{K_1 \cos(\theta/2)}{2(2\pi\rho)^{1/2}} \quad (39)$$

Equations 33 and 39 make it possible to calculate the stressed state in the case when the contour Γ is known. The contour Γ shape and size, however, depend on stress distribution themselves and have to be determined.

* The usual Kolosov–Muskhelishvily potentials notation $\varphi(z)$ and $\psi(z)$ should not be mixed with Equations 9 and 19, eigenfunctions Φ_n and Ψ_n.

To transform the equations of phase boundary equilibrium (Equation 26) the strain tensor should be divided into two items in $V^{\pm}$ regions: $u_{ik} = u_{ik}^{\pm} + u_{ik}^{*}$. u_{ik}^{*} is continuous on Γ and $u_{ik}^{\pm}$ is discontinuous on Γ strain tensor part in a corresponding region. Analogously $\sigma_{ik} = \sigma_{ik}^{\pm} + \sigma_{ik}^{*}$ in accordance with (Equation 25). With the help of Equations 28, 33 and 35 it can be obtained that

$$\sigma_{xx}^{+} = \frac{2C}{\kappa + 1}\{1 - \mathrm{Re}I'^{+}(t)\}$$

$$\sigma_{yy}^{+} = \frac{2C}{\kappa + 1}\{1 + \mathrm{Re}I'^{+}(t)\}$$

$$\sigma_{yy}^{-} = -\sigma_{xx}^{-} = \frac{2C}{\kappa + 1}\mathrm{Re}I'^{-}(t) \qquad (40)$$

Taking into account that

$$2(\lambda + \mu)u_{ll}^{+} - 2A\eta^2 = \sigma_{ll}^{+} \quad 2(\lambda + \mu)u_{ll}^{-} = \sigma_{ll}^{-} \qquad (41)$$

one can obtain $u_{ll}^{-} = 0$. Substitution of $u_{ik} = u_{ik}^{\pm} + u_{ik}^{*}$ into the phase boundary equilibria equation results in

$$\Delta f + \frac{4\mu u_0^2}{\kappa + 1} - u_0\sigma_{ll}^{*} = 0 \qquad (42)$$

where $u_0 = A_1\eta^2/2(\lambda + \mu)$ is the spontaneous deformation $u_{xx} = u_{yy} = u_0$ value of the homogeneous crystal after PT if the crystal is free of external stress. $\Delta f = f(\eta) - 2(\lambda + \mu)u_0^2$, the difference between free energy densities of phases $\eta \neq 0$ and $\eta = 0$ in such unloaded crystal.

The integral in Equation 38 turns to zero (Appendix 3). Then $\sigma_{ll}^{*} = 4\mathrm{Re}\,\varphi_{*}'(z)$. The phase boundary equation gains the form

$$\rho = \rho_0\cos(\theta/2) \quad \rho_0 = \frac{2K_I^2u_0^2}{\pi\left(\Delta f + \dfrac{4\mu u_0^2}{\kappa + 1}\right)^2} \qquad (43)$$

Equation 43 is the exact solution of the phase boundary equilibria equation.

The integral in Equation 38 becomes zero means that the nucleus existence on the crack tip does not change the stress intensity factor. It is in agreement with previous [17, 18] results and is the consequence of the well known fact that the dilatation centres do not interact due to the elastic field in the elastically isotropic media [31]. In contrast to previous results [11, 16–19] the nucleus size depends on Δf. The $\rho_0(\Delta f)$ dependence is the consequence of phase boundary equilibria equation being taken into account.

7. Transformation toughness

The metastable trail width ρ_* is not more than half of the LPT region width Fig. 5. $\rho_* \leqslant 3\sqrt{3}\rho_0/8$. Substituting Equation 43 into Equation 1 one can obtain

$$\sigma = \sigma_0 + \frac{3\sqrt{3}K_I^2u_0^2\Delta f}{4\pi\left(\Delta f + \dfrac{4\mu u_0^2}{\kappa + 1}\right)^2} \qquad (44)$$

Here from

$$K_{IC} = \frac{K_{IC}^{(0)}}{(1 - D)^{1/2}} \qquad (45)$$

here

$$D = \frac{3\sqrt{3}}{\pi}\frac{4\mu u_0^2\Delta f}{(\kappa + 1)\left(\Delta f + \dfrac{4\mu u_0^2}{\kappa + 1}\right)^2} \qquad (46)$$

and $K_{IC}^{(0)}$ is the Griffith's fracture toughness of crystal which is not undergoing PT: $K_{IC}^{(0)} = [2\sigma_0E/(1 - \nu^2)]^{1/2}$.

8. Discussion

Considering α_0 (Equation 11) in a form $\alpha_0 = \alpha'(T_0 - T_c)$, an estimation can be made for the difference of the Curie temperature T_c and the nucleation temperature T_0.

For ferroelectrics $BaTiO_3$, $PbTiO_3$ and $KTa_{1-x}Nb_xO_3$ $\alpha' \sim 10^5\,\mathrm{J\,m\,C^{-2}\,K^{-1}}$; $A/E \sim 10^{-2} - 10^{-1}\,\mathrm{m^4\,C^{-2}}$ [32], $K_{IC} \sim 0.1\,\mathrm{MPa\,m^{1/2}}$ [33], and taking usual estimation $g \sim 10^{-8}\,\mathrm{J\,m^3\,C^{-2}}$ one can obtain $T_0 - T_c \sim 10$–$100\,\mathrm{K}$.

For the nucleus size in the close overcritical regime (Equation 13) the estimation gives $r_0 \sim 10^{-8}\,\mathrm{m}$.

Estimating $k \sim 10^{-4}\,\mathrm{J\,m\,s/C^{-2}}$ (this k value corresponds to the OP relaxation time $\tau \sim 10^{-9}\,\mathrm{s}$) one can obtain for the critical speed value (23) $v_c \sim 300\,\mathrm{m\,s^{-1}}$.

An estimate of the nucleus size ρ_0 (Equation 43) for large nucleus in the far overcritical regime using experimental data for ZrO_2 $K_I \sim K_{IC} \sim 10\,\mathrm{MPa\,m^{1/2}}$ [11]; $\mu = 200\,\mathrm{GPa}$ [27]; $u_0 \sim 0.1$ [34], and supposing $\Delta f \sim \mu u_0^2$, gives $\rho_0 \sim 10^{-7}\,\mathrm{m}$. It is in agreement with the observed trail width $\rho_* \sim 0.5\,\mu\mathrm{m}$ [2] or several micrometres [1] (as well as to the nucleus size displayed in Fig. 1).

The fact that ZrO_2 as well as ferroelectrics $BaTiO_3$, $PbTiO_3$ and $KTa_{1-x}Nb_xO_3$ are improper ferroelastics is not directly considered in this paper. The estimations thus show only the qualitative agreement of the above theory to experimental data.

The estimations demonstrate that crack tip nuclei can be realized in the wide temperature region of the phase diagram. In this region boundary the anomalies of physical qualities take place. The anomalies of qualities whose values depend on the transformed crystal volume (such as the specific heat jump) are small as $V^{+} \sim r_0^2 1$. The susceptibility can, however, be observed in the vicinity of T_0. In order to calculate the susceptibility, the mass term $m\partial^2\eta/\partial t^2$ and the field $h_0f(x, y)\exp(iq_zz - iwt)$ conjugable to OP have to be added to Equation 19. (Here $f(x, y) = \exp(iq_xx + iq_yy)$.) The main term of susceptibility has the form

$$\chi_{q,w} = \frac{(f(x, y), \Psi_0)(\Psi_0, \Psi_0)^{-1}}{\alpha - \alpha_0 + gq_z^2 - mw^2 - ikw} \qquad (47)$$

if $\alpha > \alpha_0$. $(f, \Psi_0) = \int f\Psi_0\,dx\,dy$. (Particularly in the case $\boldsymbol{q} = (0, 0, q_z)$ $f = 1$, (f, Ψ_0) $(\Psi_0, \Psi_0)^{-1} \approx 12.7$.) The susceptibility has an anomaly near the nucleation temperature T_0.

The existence of the nucleus on the crack tip, in the phase diagram region where metastable trail cannot

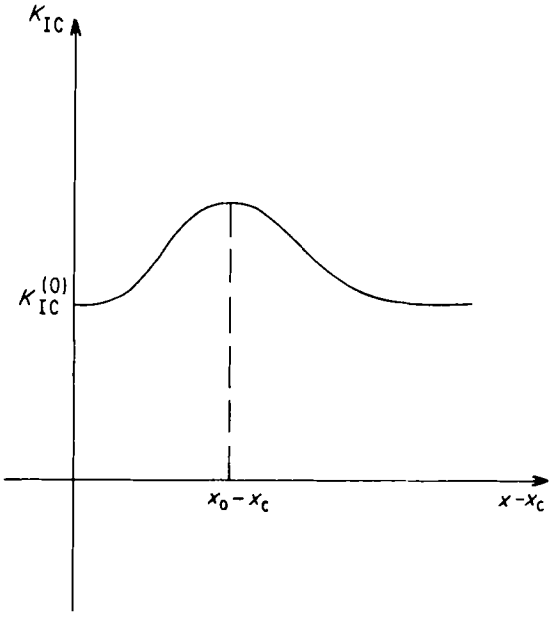

Figure 6 The transformation toughness concentration dependence.

arise, decreases the fracture toughness. Using the additional K_I term ΔK_I (Equation A2.8) one can obtain

$$K_{IC} = K_{IC}^{(0)}(1 + R\xi^2)^{-1} \quad (48)$$

which decreases with increasing ξ thus the field, h, which is conjugated to OP results in the crystal cracking if $K_I < K_{IC}^{(0)}$. Using results Equations 47 and 48, averaging ΔK_I and considering the OP amplitude χh_0 to be small, one can obtain

$$K_{IC} \approx K_{IC}^{(0)}(1 - R|\chi h_0|^2(f, \Psi_0)^2) \quad (49)$$

Fracture toughness (Equation 49) is a minimum in the nucleation point T_0.

The transformation toughening phenomenon is the result of a metastable trail arising and can realize only in two-phase region of phase diagram (double shaded region in Fig. 2).

D (Equation 46) is a maximum if $\Delta f = 4\mu u_0^2/(\kappa + 1)$ and vanishes on the boundary of two-phase region, $D_{max} = 3\sqrt{3}/4\pi$. It results in $(K_{IC}/K_{IC}^{(0)})_{max} \approx 1.3$. Considering $\Delta f = b(x - x_c)$ (here is a concentration of a dissolved matter, x_c – its concentration at the PT point) one can obtain $K_{IC}(x)$ dependence (Fig. 6) (with maximum point $x_0 = x_c + 4\mu u_0^2/b(\kappa + 1)$ which is in the region of stability of the phase $\eta = 0$). This $K_{IC}(x)$ dependence is in a qualitative agreement with the experimental one for $(ZrO_2)_{1-x}(Y_2O_3)_x$ [10, 20].

Appendix 1. The Equation 9 solution

The scale transformation $x = r_0 x_1$, $y = r_0 y_1$ results (Equation 9) in a two-dimensional Shrödinger equation

$$\Delta\Psi + \frac{\cos(\theta/2)}{\sqrt{\rho}}\Psi = \varepsilon^2\Psi \quad (A1.1)$$

where $\Delta = \partial^2/\partial x_1^2 + \partial^2/\partial y_1^2$; $\rho = (x_1^2 + y_1^2)^{1/2}$.

The solution of (Equation A1.1) of the form $\Psi = \exp(-\varepsilon\rho)f(z)$ should be tried, where $z = \rho^{1/2}\cos(\theta/2)$. The equation for $f(z)$ is

$$f'' - 4\varepsilon z f' - 4(\varepsilon - z)f = 0 \quad (A1.2)$$

The transformation $f = \varphi(x)\exp(z/\varepsilon)$; $x = [z - (2\varepsilon^2)^{-1}](\varepsilon/2)^{1/2}$ gives

$$\varphi'' - 2x\varphi' + \lambda\varphi = 0 \quad (A1.3)$$

the Hermitian polynomial equation, $\lambda = 2[1 - (4\varepsilon^3)^{-1}]$. The spectrum condition is $\lambda = 2n$; $n = 0, 1, 2, 3 \ldots$ It is not difficult to see that (Equation A1.1) has only ground bounded state $n = 0$, $\varepsilon_0 = 4^{-1/3}$.

Appendix 2. The nucleus state equation and Ω-potential calculation

Considering the last term in (Equation 6) as the bulk force field one can obtain

$$u_{ik} = u_{ik}^{(0)} + u_{ik}^{(1)} \quad (A2.1)$$

where

$$u_{ik}^{(1)} = A\int G_{ij}(\boldsymbol{q})q_j q_k \tilde{Q}(\boldsymbol{q})\exp(i\boldsymbol{qr})\frac{d^3q}{(2\pi)^3} \quad (A2.2)$$

$\tilde{Q}(\boldsymbol{q}) = 2\pi\delta(q_z)Q(q_x, q_y)$; $Q(q_x, q_y) = \int\eta^2(x, y)\exp(i\boldsymbol{qr})\,d^2r$ is the Fourier image of the OP square, $G_{ij}(\boldsymbol{q})$ the Fourier image of the Green function of elastically isotropic infinite media

$$G_{ik}(\boldsymbol{q})q_j q_k = \frac{1 - 2\nu}{2\mu(1 - \nu)}\frac{q_i q_j}{\boldsymbol{q}^2} \quad (A2.3)$$

Using Equations A2.1 to A2.3 one can obtain

$$\sigma_{yy}^{(1)} = (\lambda_0 + 2\mu)u_{ll}^{(1)} - 2\mu u_{xx}^{(1)}$$

$$\sigma_{yy}^{(1)} = \frac{A(1 - 2\nu)(\lambda_0 + 2\mu)}{2\mu(1 - \nu)}\eta^2$$

$$- \frac{A(1 - 2\nu)}{(1 - \nu)}\int\frac{q_x^2}{\boldsymbol{q}^2}Q(\boldsymbol{q})\exp(i\boldsymbol{qr})\frac{d^2q}{(2\pi)^2} \quad (A2.4)$$

The boundary condition on the crack L gains the form

$$\sigma_{yy}^{(0)} + \sigma_{yy}^{(1)} = -p(t) \quad t \in L \quad (A2.5)$$

it gives

$$\sigma_{ik}^{(0)} = \frac{K_{Ieff}}{(2\pi r)^{1/2}}f_{ik}(\theta) \quad K_{Ieff} = K_I + \Delta K_I \quad (A2.6)$$

where K_I is given by the expression (Equation 8) and $\Delta K_I = \Delta K_I' + \Delta K_I''$:

$$\Delta K_I' = -\frac{A(1 - 2\nu)}{(1 - \nu)(\pi a)^{1/2}}\int_{-a}^{a}dx\left(\frac{a + x}{a - x}\right)^{1/2}$$

$$\times\int\frac{q_x^2}{\boldsymbol{q}^2}Q(\boldsymbol{q})\exp(iq_x x)\frac{d^2q}{(2\pi)^2} \quad (A2.7)$$

$$\Delta K_I'' = \frac{A(1 - 2\nu)(\lambda_0 + 2\mu)\xi^2}{2\mu(1 - \nu)s_2(0)(\pi a)^{1/2}}\int_{-a}^{a}\left(\frac{a + x}{a - x}\right)^{1/2}$$

$$\times\exp\left(-\frac{2|x - a|}{4^{-1/3}r_0}\right)dx \quad (A2.8)$$

Considering the case $a \gg r_0$ and making the numerical

calculation of the integral (Equation A2.7) one can obtain

$$\Delta K_I = R\xi^2 K_I \quad \text{(A2.9)}$$

$$R \approx 0.026 \frac{A^2(1-2\nu)^2(1+\nu)}{Eg(1-\nu)}\left(1 + 0.46\frac{1-\nu}{1-2\nu}\right) \quad \text{(A2.10)}$$

In order to obtain the branching equation for system (Equation 6) one has to eliminate u from the first Equation 6 using Equations A2.1, A2.2, A2.6 and A2.7 and display equation in a form

$$g\Delta\eta - \left(\alpha_0 - B\frac{\cos(\theta/2)}{\sqrt{r}}\right)\eta = (\alpha - \alpha_0)\eta + \left(\beta - \frac{A^2(1-2\nu)}{\mu(1-\nu)}\right)\eta^3 - \frac{2A\Delta K_I \cos(\theta/2)}{\lambda_0 + \mu\,(2\pi r)^{1/2}}\eta + \gamma\eta^5 \quad \text{(A2.11)}$$

The condition of existence of a solution of Equation A2.11 is the orthogonality of the right-hand part of Equation A2.11 to the eigenfunction of Equation 9 [21]. Substituting $\eta = \xi\Psi_0$, ΔK_I (Equations A2.9 and A2.10) into Equation A2.11 one can obtain the branching equation which is the equation of state of the crack tip nucleus

$$(\alpha - \alpha_0)\xi + 0.018\tilde{\beta}\xi^3 + 0.00048\gamma\xi^5 = 0 \quad \text{(A2.12)}$$

The equation of state must result from the minimum condition of the Ω-potential, describing the transition from the state without the nucleus ($\xi = 0$) to the state with nucleus on the crack tip ($\xi \neq 0$). Integrating Equation A2.11 one obtains Equation 14. The potential (Equation 23) can be obtained analogously. The integrals $s_n(\delta)$ are calculated numerically. The results for different values of δ are given in Table I.

Appendix 3. Calculation of the integral $I(z)$ contribution

The calculation of the contribution of Equation 35 to Equation 38 is made for the case $\rho_0/a \ll 1$ – the crack is considered to be semi-infinite, it right end in the co-ordinate origin. The conformal transformation $z = \rho_0(\xi + 1)^2/4$ turn the contour of cardioid Γ into the contour of unit circle γ, the points of the crack contour $z = -x + i0$ into $\xi = -1 + iy$, and points $z = -x - i0$ into $\xi = -1 - iy$ Fig. 7a and b. $I(z)$ gains the form

$$I(\xi) = \frac{\rho_0}{4\pi i}\oint_\gamma \frac{(\sigma+1)^3\,d\sigma}{\sigma^2(\sigma+\xi)(\sigma+\xi+2)} \qquad |\sigma| = 1 \quad \text{(A3.1)}$$

and it is calculated along the unit circle contour γ. Considering $\mathrm{Re}\,\xi = -1$ one can calculate the Equation A3.1 values on the crack contour $\xi = -1 \pm iy$ and after

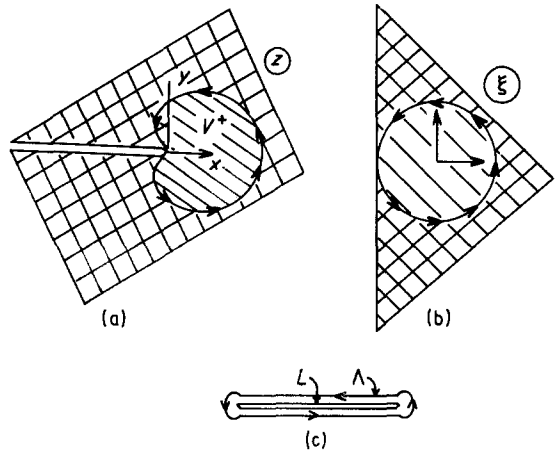

Figure 7 Calculation of $I(z)$ and its contribution to stress intensity. (a) The conformal transformation of the cardioid interior V^- into the plane part $\mathrm{Re}\,\xi \geqslant -1$ which lies outside of unit circle. (c) Calculation of the integral $J(z)$. L is the crack contour and Λ the contour of integration.

the transformation to the z plane can obtain

$$I(x) = \frac{3\rho_0}{2(1-4x/\rho_0)} - \frac{\rho_0}{(1-4x/\rho_0)^2} \quad (x < 0) \quad \text{(A3.2)}$$

Calculation of the integral (Equation 38) now can be made exactly. It has to be taken along the contour Λ (Fig. 7c). The integral

$$J(z) = \frac{1}{2\pi i}\int \frac{(t^2 - a^2)^{1/2}}{t - z} I'(t)\,dt \quad \text{(A3.3)}$$

is equal to the half of the difference of $(z^2 - a^2)^{1/2} I'(z)$ and its singular part, which is

$$\frac{\rho_0}{4}(a\rho_0)^{1/2}\left(\frac{\rho_0^2}{2(z - a - \rho_0/4)^3} + \frac{5\rho_0}{2(z - a - \rho_0/4)^2} - \frac{2}{z - a - \rho_0/4}\right) \quad \text{(A3.4)}$$

$J(a)$ takes place in Equation 38. It is not difficult to see now that $J(a) = 0$. The elastic imagination forces do not thus give any contribution to Equation 38.

Acknowledgements

It is a pleasure to thank Dr. V. I. Isotov, who kindly gave a photo, Fig. 1 for publication; Dr A. L. Roitburd and Dr A. L. Korzhenevski for the discussions and M. L. Kraizman for his help with the numerical calculations.

References

1. D. L. PORTER and A. H. HEUER, *J. Amer. Ceram. Soc.* **60** (1977) 183.
2. L. K. LENZ and A. H. HEUER, *ibid.* **65** (1982) 192.
3. V. G. GARIN, *Sverhtverdie materiali* **2** (1982) 17.
4. E. HORNBOGEN, *Acta Metall.* **26** (1978) 147.
5. S. O. KRAMOROV, N. Ya. YEGOROV and L. M. KANTSEL'SON, *Fiz. Tverdogo Tela* **28** (1986) 2858.
6. V. K. VLASKO-VLASOV, L. M. DEDUH, M. V. INDENBOM and V. I. NIKITENKO, *Zh. Eksp. Teor. Fiz.* **84** (1983) 277.

7. V. K. VLASKO-VLASOV and M. V. INDENBOM, *ibid.* **86** (1984) 1084.
8. M. V. BELOUSOV and B. E. VOLF, *Zh. Eksp. Teor. Fiz. Lett.* **31** (1980) 348.
9. S. N. ZOLOTAREV, I. B. SIDOROVA, Yu. A. SKAKOV and V. A. SOLOV'EV, *Fiz. Tverdogo Tela* **20** (1978) 775.
10. R. P. INDEL, R. W. RICE and D. LEVIS, *J. Amer. Ceram. Soc.* **65** (1982) 108.
11. T. K. GUPTA, F. F. LANGE and J. H. BEHTOLD, *J. Mater. Sci.* **13** (1978) 1464.
12. P. F. BEHER and V. J. TENNERY, "Fracture Mechanics of Ceramics" Vol. 6 (Plenum, New York, 1983) p. 383.
13. N. CLAUSSEN, *Z. Werkstoffitechnic* **13** (1982) 138.
14. V. N. VAR'UHIN, A. T. KOZAKOV, V. A. DEM'JANCHENKO and S. I. SHEVTSOVA, *Superconductivity* **2** (1989) 26.
15. N. F. MOROZOV, "Matematicheskie Voprosi Teorii Treshin" (Nauka, Moscow, 1984).
16. S. D. ANTOLOVICH, *Trans. Met. Soc. AIME* **242** (1968) 2371.
17. R. M. McMEEKING and A. G. EVANS, *J. Amer. Ceram. Soc.* **65** (1982) 242.
18. B. BUDIANSKI, J. M. HUTCHINSON and J. M. LAMBROPOULOS, *Int. J. Solid Structures* **19** (1983) 337.
19. F. F. LANGE, *J. Mater. Sci.* **17** (1982) 235.
20. *Idem., ibid.* **17** (1982) 240.
21. M. M. VAINBERG and V. A. TRENOGIN, "Teoria Vetvlenia Reshenii Nelineinih Uravnenii" (Nauka, Moscow, 1969).
22. V. Z. PARTON and V. G. BORISOVSKI, "Dinamicheskaja Mechanika Razrushenija" (Mashinostrojenije, Moscow, 1985).
23. A. L. ROITBURD, *Usp. Fizi. Nauk* **113** (1974) 69.
24. *Idem., Fiz. Tverdogo Tela* **26** (1984) 2025.
25. F. IONA and D. SHIRANE, "Segnetoelectricheskije Kristalli" (Mir, Moscow, 1965).
26. LANDOLT-BORNSTEIN, "Zahlenwerte und Functionen aus Naturwissenshaften und Technik" edited by K. N. Hellweg Vol. 3. "Kristall und Festkorperphysic" (Springer-Verlag, 1982).
27. D. MISHEL, L. MAZEROLLES, M. PEREZ and Y. JORBA, *J. Mater. Sci.* **18** (1983) 2618.
28. A. A. BUL'BICH, *J. Techn. Phys. Lett.* **12** (1986) 645.
29. *Idem., Metallophizika* **9** (1987) 88.
30. N. I. MUSKHELISHVILY, "Nekotirije Osnovnije Zadachi Matematicheskoi Teorii Uprugosti" (Nauka, Moscow, 1966).
31. J. D. ESHELBY, *Solid State Phys.* **3** (1956) 79.
32. E. G. FESENKO, V. G. GAVRIL'ACHENKO and A. F. SEMENCHEV, *Domennaja Struktura Mnogoosnih Segnetoelectricheskih Kristallov.* Rostov-on-Don University, Rostov-on-Don (1990).
33. R. C. POHANKA, S. W. FREIMAN and B. A. BENDER, *J. Amer. Ceram. Soc.* **61** (1978) 72.
34. LI CHUNG MING and M. H. MANGHNANI, *Mater. Res. Soc. Symp. Proc.* **22** (1984) 81.

Received 1 November 1990
and accepted 25 March 1991